Korean J. Chem. Eng., 33(7), 2205-2214 (2016)
DOI: 10.1007/s11814-016-0061-2

pISSN: 0256-1115
eISSN: 1975-7220

Continuous biosorption of U(VI) and Fe(II) using *Cystoseira indica* biomass packed bed column: Breakthrough curves studies in single, binary and multi-component systems

Ali Talebian*, Ali Reza Keshtkar,†, and Mohammad Ali Moosavian***

*Department of Chemical Engineering, Faculty of Engineering, University of Tehran, Tehran, Iran
**Nuclear Fuel Cycle School, Nuclear Science and Technology Research Institute, Tehran, Iran
(*Received 14 December 2015 • accepted 25 February 2016*)

Abstract−Ca-pretreated *Cystoseira indica* algae was used as a biosorbent for the biosorption of U(VI) and Fe(II) ions in single, binary and multi-component systems by using a packed bed column. Experiments were conducted to study the effect of important design parameters such as bed height and flow rate. FTIR and XRF analyses and pH and Ca^{2+} ion concentration recordings showed that the biosorption of U(VI) and Fe(II) proceeded through ion-exchange mechanism. BDST, Thomas and Modified dose-response models were used for predicting breakthrough curves and for estimations of the parameters necessary for the design of a large-scale packed bed column.

Keywords: Biosorption Mechanism, U(VI), Fe(II), Packed Bed Column, *Cystoseira indica* Algae

INTRODUCTION

The separation and recovery of valuable radionuclides and heavy metals from aqueous solution have acquired great significance. Uranium is the most vital element for nuclear energy programs and is available in the leach solution of various uranium ores as well as in the uranium chemical conversion facilities effluents. Leaching is a process through which the ore is placed in contact with a suitable solvent; as a result, some components of the ore minerals are dissolved in it. This leaching process produces vast quantities of complex, dilute uranium solution and a variety of other heavy metal ions such as iron due to the characteristics of the ore mines.

Different procedures such as chemical precipitation [1], membrane separation [2], electrochemical treatment [3], reverse osmosis [4], solvent extraction [5] and ion-exchange [6] can be used for heavy metal separation and recovery from aqueous solution. These common technologies suffer from some restrictions such as high operational and capital costs, incomplete metal removal, weak selectivity, high energy consumption and the generation of toxic slurries [3]. Biosorption represents an alternative to conventional processes. It can be used to describe the adsorption of heavy metals from an aqueous solution by a passive binding to non-living biomass [7]. Biosorption has many advantages including low capital and operating costs, selective removal of metals, biosorbent regeneration and metal recovery potentiality and being absolutely free from sludge generation [8]. Generally, metal biosorption includes complex mechanisms of ion exchange, chelation, adsorption by physical forces, and ion entrapment in inter- and intrafibrillar capillaries and spaces of the cell structural network. Several similar studies showed that non-living microorganisms can be effective in the adsorption of heavy metal ions such as blue-green algae [9,10], red algae [11,12] and brown algae [8,13,14]. The biomass used in this work, *Cystoseira indica*, brown algae was obtained from the coast of Chabahar, Iran. For increasing the metal loading capacity of biosorbent, raw algae can be pretreated with calcium solution. This process will result in a change in surface ions and will increase the biomass biosorption capacity in comparison with untreated algae, since the biosorption is usually an ion exchange process [15].

Although equilibrium batch adsorption studies provide useful information on the application of adsorption, most separation and purification processes that employ sorption technology use continuous flow columns. High driving force (due to concentration gradient), which improves biosorption efficiency and mass transfer performance, is an important feature of the continuous flow system [16]. Operating conditions such as pH, feed concentration, volumetric flow rate and bed height are key process parameters, which could be used for comparison, process design, and scale-up purposes. The dynamic behavior of a continuous flow column is evaluated in terms of breakthrough curve (effluent solute concentration versus time) [17].

Mathematical modeling of data available from sorption process facilitates scale-up potential and is necessary for optimal process design and operation. Also, biosorption process modeling is useful for predicting the process performance under different conditions. Hence, several models, namely Thomas [18], Modified dose-response [19] and Bed Depth Service Time (BDST) [20] have often been used in the studies; the first two models predict the service time for a given metal ion concentration and the information thus obtained is useful in the BDST model to predict bed height.

The main objective of this study was to investigate the biosorption of U(VI) from single, binary and multi-component systems

†To whom correspondence should be addressed.
E-mail: akeshtkar@aeoi.org.ir

including U(VI) and Fe(II) in a packed bed column by the Ca-pretreated *C. indica* algae biomass. The effects of operational conditions such as bed height, flow rate and presence of interfering ions were examined. For a suitable design of the biosorption column, an accurate prediction of the breakthrough curve is needed. Hence, the experimental data obtained from the continuous flow systems were fitted to the above-mentioned models for U(VI) biosorption. Also, biosorption mechanism was investigated by FTIR and XRF analyses before and after biosorption and by recording the Ca(II) ion and pH of column effluent stream.

MATERIALS AND METHODS

1. Preparation of Biosorbent

C. indica brown algae used in the experiments was obtained from the coast of Chabahar, Iran. After being rinsed thoroughly and frequently with deionized water, it was sun dried. The samples were crushed and sorted using a sieve to select the batch of biomass with particle size of 1-2 mm. Since our previous study illustrated that the uptake capacity of uranium by calcium pretreated *C. indica* was greater than raw *C. indica* algae [15], the selected biomass was treated with 0.1 M $CaCl_2{\cdot}2H_2O$ solution for more active binding sites embedded in the cell wall and removal of surface impurities. Pretreatment of *C. indica* was undergone by adding 10 g biomass to 0.1 M $CaCl_2{\cdot}2H_2O$ solution (1,000 mL) in the batch system. Then, it was stirred slowly for 3 h at 150 rpm and 25 °C. Next, pretreated biomass was rinsed several times with deionized water to remove excess calcium ions. Finally, the Ca-pretreated biomass was dried in an oven at 70 °C overnight.

2. Stock Solutions of Metal Ions

A stock solution of U(VI) with a concentration of 0.5 g L^{-1} was prepared by the use of deionized water and analytical grade salts of $UO_2(NO_3)_2{\cdot}6H_2O$ (Sigma-Aldrich). A stock solution of Fe(II) with a concentration of 1.8 g L^{-1} was prepared by utilizing deionized water and analytical grade salts of $FeCl_2{\cdot}4H_2O$ (Sigma-Aldrich). The working solutions of mono-metal ions were prepared by diluting stock solutions of mono-metal ions with deionized water. The working solutions of binary-metal ions were prepared by mixing one liter of each stock solution of mono-metal ions. The initial metal concentrations were 250 and 900 mg L^{-1}, respectively for U(VI) and Fe(II) in single and binary-metal ion systems. The multi-component solutions were prepared by dissolving the weighed amounts of uranyl nitrate, iron chloride, zinc chloride, cerium chloride, yttrium chloride, ytterbium chloride, lanthanum chloride, nickel nitrate, copper nitrate and cobalt nitrate (Sigma-Aldrich) in deionized water. All experiments were performed at 25 °C and an initial pH of 4. This pH value was considered as the optimum pH value for U(VI) biosorption [15]. The pH of solutions was measured with a pH meter (Metrohm, Model 780) and adjusted by using 0.1 M HCl and/or 0.1 M NaOH. The samples collected periodically were analyzed for the remaining U(VI) and Fe(II) ions concentration by an inductively coupled plasma spectroscopy (ICP, Varian, Model Liberty 150 AX Turbo).

3. Operation of Packed Bed Column and Instrumentation

A glass column with an internal diameter of 1.5 cm and a length of 10 cm was employed in the column experiments. Columns were packed with modified biosorbent and for supporting the biosorbent in the column, glass wool (1 cm depth) was fitted onto the two ends of the column. The metal solution was passed through the column in upward direction with the help of peristaltic pump (Watson Marlow Pumps, Model 205U). To obtain biosorption equilibrium data, the experiments were performed in the packed bed column to complete biosorbent saturation. Note that the saturation occurs when the outlet metal concentration reaches a constant value (equal to the inlet concentration).

FTIR and XRF were analyzed to find the main biosorption mechanism. FTIR spectra of Ca-pretreated biomasses and biomasses loaded with U(VI) and Fe(II) were taken by a Bruker Vector 22 FTIR spectrometer in the region of 400-4,000 cm^{-1}. Also, Ca-pretreated biomasses and biomasses loaded with U(VI) and Fe(II) were analyzed using an X-ray fluorescence analyzer (XRF) Model ED 2000 Oxford Instruments Corporation.

4. Modeling and Analysis of Column Data

Packed bed biosorption studies are usually explained through the concept of the S-shaped experimental curves called breakthrough curves, which are plotted as outlet concentration (C_t)/ input concentration (C_0) vs. time. The breakthrough curves have very important characteristics for process design and determining the operation life span of the bed and the dynamic response of biosorption in a packed bed column, because they directly affect the feasibility and economics of the sorption phenomenon. Column operating conditions such as inlet concentration, flow rate and bed height are very effective on experimental breakthrough curves [15].

The breakthrough time (t_b, the time at which metal concentration in the effluent reaches 5% of the influent value) and bed exhaustion time (t_e, the time at which metal concentration in the effluent exceeds 95% of the influent value) were determined to characterize the breakthrough curves [15].

The uptake capacity (q_{total}) of the biosorbent by the column was calculated as follows:

$$q_{total} = \frac{C_0 Q}{1000 \times m_s} \int_0^{t_e} \left(1 - \frac{C_t}{C_0}\right) dt \quad (1)$$

where q_{total} is the amount of metal removed (mg metal g^{-1} biosorbent), C_0 is the influent metal concentration (mg L^{-1}), C_t is the effluent metal concentration at time of t (mg L^{-1}), Q is the volumetric flow rate (mL min^{-1}), m_s is the amount of dried biosorbent packed in the column (g) and t is the time (min).

The effluent volume (Ve) can be calculated as follows [15]:

$$V_e = Q \times t_e \quad (2)$$

The total amount of metal sent to column (M_{total}) can be calculated as follows [15]:

$$M_{total} = \frac{Q \times C_0 \times t_e}{1000} \quad (3)$$

The removal efficiency (% RM) of metal at saturation of the column was calculated as follows [13]:

$$\% \text{ RM} = \frac{m_s \times q_{total}}{M_{total}} \times 100 \quad (4)$$

BDST is one of the most commonly used models to describe and

design the heavy metals sorption by means of the packed bed system. This model, regardless of inter-particle resistance and resistance to foreign film, is defined on the basis of the surface reaction and assumes that the metal ions are directly absorbed on the adsorbent surface [21]. The BDST equation expresses a linear relationship between the bed height (Z) and breakthrough time, in terms of process concentrations and adsorption parameters, often called service time at the bed, given by:

$$t_b = \frac{N_0 Z}{C_0 v} - \frac{1}{K_a C_0} \ln\left(\frac{C_0}{C_b} - 1\right) \quad (5)$$

where N_0 is the biosorption capacity of the bed (mg L^{-1}), K_a is the rate constant (L mg^{-1} min^{-1}), C_b is breakthrough ion concentration (mg/L) and v is the linear velocity calculated by dividing the flow rate by the column section (cm min^{-1}). The value of biosorption capacity of the bed and the rate constant were computed from the slope and intercept of BDST plot assuming initial concentration and the linear velocity as constant. The bed biosorption capacity shows the time required for the adsorption zone to move a unit length through the biosorbent, and the rate constant shows the rate of solute transfer from the liquid phase to the solid phase. If Ka is small, a long bed will be required to delay breakthrough, but as Ka increases, a progressively smaller bed is needed to delayed breakthrough [22].

The Thomas model has been mostly used to describe the performance of the sorption process in a packed bed column. Also, this model has been used to predict the breakthrough curve of metal sorption by several investigators [8,15,18]. The same model derived from equation of mass conservation in a flow system [23] assumes that the adsorption equilibrium follows the Langmuir model kinetics of adsorption–desorption without any axial dispersion in the adsorption column with the assumption that the rate of driving force obeys second-order reversible reaction kinetics [20,24]. The expression by Thomas for an adsorption column is given as follows:

$$\frac{C}{C_0} = \frac{1}{1 + \exp\left(\frac{M q_0 k_{Th}}{Q} - \frac{V C_0 k_{Th}}{Q}\right)} \quad (6)$$

where V is the volume (*l*) of metal solution passed into the column, k_{Th} is the Thomas rate constant (L min^{-1} g^{-1}), q_0 is the maximum uptake capacity (mg g^{-1}). The model parameters k_{Th} and q_0 can be estimated by non-linear fitting of Eq. (6) to the experimental data of breakthrough curves.

Yan et al. [19] have proposed the modified dose-response model for the modeling of breakthrough curves of the packed column metal biosorption process. This model minimizes the error that results from the use of the Thomas model, especially with lower and higher breakthrough curve times [25].

$$\frac{C}{C_0} = 1 - \frac{1}{1 + \left(\frac{V}{b_{mdr}}\right)^{a_{mdr}}} \quad (7)$$

where a_{mdr} and b_{mdr} are the modified dose-response model constants.

All the above-mentioned models were fitted to the experimental breakthrough curves using the non-linear regression method, and their suitability was assessed on the basis of R^2.

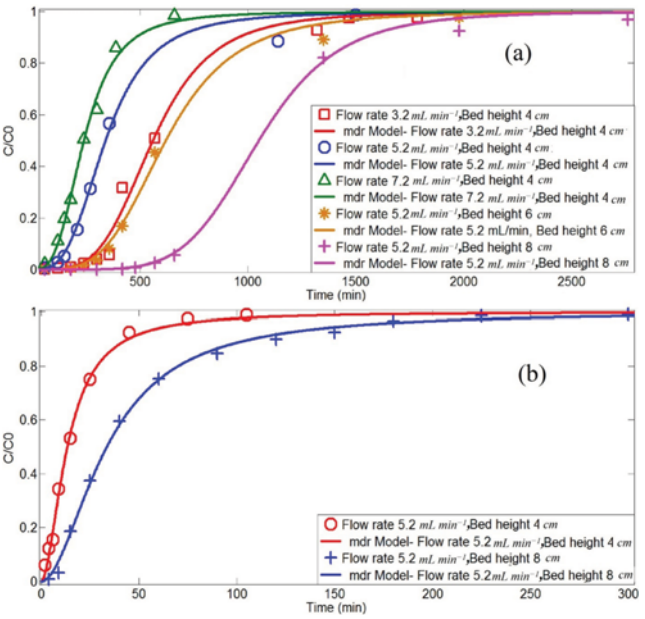

Fig. 1. Comparison of the experimental and predicted breakthrough curves for (a) U(VI) and (b) Fe(II) biosorption from single-component system by Ca-pretreated *C. indica* at different bed heights and flow rates according to the Modified dose-response model (initial uranium(VI) concentration=250 mg l^{-1}; initial iron(II) concentration=900 mg l^{-1}; pH 4).

RESULTS AND DISCUSSION

1. Study of Biosorption from Single Metal Solutions

To evaluate the performance of continuous biosorption process, the flow rate plays an important role. The influence of flow rate on the biosorption of U(VI) by Ca-pretreated *Cystoseira indica* algae was investigated by keeping the influent metal concentration (250 mg L^{-1}) and the bed height (1 cm) constant and varying the flow rate (3.2, 5.2 and 7.2 mL min^{-1}).

The results of experiments on the effect of flow rate are shown in Fig. 1(a), and the results of the breakthrough curve analysis are given in Table 1. The results show that the breakthrough time decreases from 333 to 78 min, as flow rate increases from 3.2 to 7.2 mL min^{-1}, also the breakthrough curve becomes steeper. This is because in the high flow rate of the solution the residence time of the solute in the column is not enough to progress mass transfer and U(VI) ions escape the column before the equilibrium is attained. The removal efficiency of U(VI) for the packed bed biosorption column was found to decrease from 51.51% to 28.86% with an increase in the flow rate. It was because the contact time for U(VI) biosorption was very short at higher flow rates. The results indicate that the uptake capacity value increased from 337.29 to 363.87 mg g^{-1} with increasing the flow rate from 3.2 to 5.2 mL min^{-1}. Then it reduced to value 286.61 mg g^{-1} in the flow rate 7.2 mL min^{-1}. Two important factors could be effective on the amount of uptake capacity.

With an increase in the flow rate, disturbances (mixing) as the

Table 1. Column data and parameters obtained for single, binary and multi-component systems

Experimental conditions			Experimental parameters of breakthrough curve				
Metal	Flow rate (ml/min)	Bed height (cm)	t_b (min)	t_e (min)	Uptake capacity (mg g^{-1})	Uptake capacity from mdr model	%RM
Single system							
U(VI)	3.2	4	333	1390	337.29	321.44	51.51
	5.2	4	148	1370	363.87	339.21	36.11
	7.2	4	78	532	286.61	288.74	28.86
	5.2	6	319	1784	381.14	368.29	41.01
	5.2	8	643	2440	433.03	415.79	45.28
Fe(II)	5.2	4	-	60	55.18	54.98	33.33
	5.2	8	10	168	73.49	72.23	30.75
Binary system							
U(VI)	3.2	4	37	1103	165.31	168.05	31.21
	5.2	4	34	1056	223.58	225.63	28.16
	7.2	4	20	515	199.95	208.52	37.74
	5.2	6	69	1552	227.14	245.89	27.82
	5.2	8	87	2496	257.21	241.37	27.95
Fe(II)	5.2	4	-	44	54.84	56.14	44.94
	5.2	8	6.5	108	62.04	64.11	41.53
Multi-component system							
Bandar Abbas leach solution, U(VI)	5.2	8	38	1220	130.05	129.19	29.29
Saghand leach solution, U(VI)	5.2	8	5.5	201	30.09	32.01	40.12

first factor increase and the thickness of the liquid film surrounding the *C. indica* biosorbent particle as a resistance for the mass transfer decreases. Thus, reducing the film transfer resistance, increases in the mass transfer rate and this factor causes the growth of the uptake capacity by increasing the flow rate from 3.2 to 5.2 mL min^{-1}. On the other hand, by increasing the flow rates, the retention time for U(VI) ions to interact with the biosorbent as the second factor decreases and U(VI) ions have little time to diffuse into the biosorbent sites or pores through intra-particle diffusion. In this case, the U(VI) metal ion uptake is limited by internal mass transfer. This factor can be the cause of the uptake capacity reduction by the increasing flow rate from 5.2 to 7.2 mL min^{-1}. The same observations have been reported elsewhere [15,26]. So, the flow rate 5.2 mL min^{-1} was selected as the optimum flow rate for further experiments.

The influence of changing bed height on biosorption of U(VI) in the packed bed column was also investigated at flow rate 5.2 ml min^{-1} and initial concentration of U(VI) 250 mg L^{-1} and the results of which are shown in Fig. 1(a). The mass for 4, 6 and 8 cm of bed heights was about 1.75, 2.62 and 3.5 g of Ca-pretreated *C. indica*, respectively. The influence of bed height was well pronounced in terms of breakthrough time (t_b) and exhaustion time (t_e), as both increased with an increase in the bed height (Table 1). The biosorption capacity of U(VI) increased with an increase in the bed height from 363.87 mg g^{-1} to 433.03 mg g^{-1}, which could be due to an increase in the residence time of the U(VI) ions and also provided more number of binding sites and ionic groups of biomass available for biosorption of U(VI) metal ions [27]. On the other hand, at the low bed height, axial dispersion phenomena predominated in the mass transfer, reduced the diffusion of metal ions [28].These results are in agreement with that reported ones by other researchers [15,29].

Considering that the main objective of this work was U(VI) biosorption as a more precious metal from real solutions, the biosorption of Fe(II) was studied in the optimal conditions of U(VI) biosorption. Fig. 1(b) illustrates the breakthrough curves of Fe(II) at initial concentration 900 mg L^{-1} and flow rate 5.2 ml min^{-1} and bed heights 4 and 8 cm. As seen, the breakthrough time and uptake capacity values for Fe(II) biosorption are smaller than those of U(VI) biosorption in similar conditions (Table 1). Higher uptake capacity of U(VI) than that of Fe(II) was just in agreement with the greater affinity of U(VI) than that of Fe(II) for binding to active sites of Ca-pretreated *C. indica* algae. The binding strength of a metal ion to the biomass is dependent upon other different factors such as some physical and chemical properties of U(VI) and Fe (II) ions.

This might be attributed to the difference between the ionic radius of UO_2^{2+} (102.5 pm) and Fe^{2+} (78 pm). The ionic radius of U(VI) ions is larger than that of Fe (II) and thus a stronger physical affinity for U(VI) is expected at the adsorption sites on the cells [30].

Moreover, higher atomic weight of UO_2^{2+} ions generated higher momentum energy, which to the best of our knowledge, could be helpful for help of the U(VI) biosorption by increasing the probability of effective encounter between U(VI) and the cellular walls [31].

Also, the Pauling electronegativity of U(VI) is 1.38 while the Pauling electronegativity of Fe(II) is 1.83. the higher electronegativity, the lower binding tendency of metal ions to the negative sites on algae will be resulted [18].

Another factor that influenced the biosorption capacity of metal ions was the ability of metals to form hydroxy complexes in aqueous solutions. Hydrolysis reactions of U(VI) and Fe (II) metal ions can be expressed by the following equations.

$$UO_2^{2+}+H_2O=UO_2OH^++H^+ \qquad pK=5.8 \qquad (8)$$

$$Fe^{2+}+H_2O=FeOH^++H^+ \qquad pK=9.5 \qquad (9)$$

Lower hydrolysis constant (pK) value will lower the degree of solvation of metal ions; thus the metal ion can diffuse easily and has a stronger binding strength. Since U(VI) has a lower pK, there is a lower resistance to reach the active sites of the Ca-pretreated *C. indica* algae [32].

2. Study of Biosorption from Binary Metal Solutions

Continuous column studies were carried out to observe metal uptake by Ca-pretreated *C. indica* algae at three different flow rates of 3.2, 5.2 and 7.2 mL min^{-1} and bed heights of 4, 6 and 8 cm from the binary metal ion system comprising of U(VI) and Fe(II) with inlet concentration 250 and 900 mg L^{-1}, respectively. The breakthrough curves of the U(VI) biosorption from binary mixtures for various flow rate are plotted in Fig. 2(a) and analysis results are summarized in Table 1. As expected, with the increasing flow rate, the breakthrough curves are steeper and the breakthrough time decreases. In addition, with an increase in the flow rate from 3.2 to 5.2 mL min^{-1} mixing increases and the thickness of the liquid film surrounding the biosorbent particle decreases and consequently the mass transfer rate increases. On the other hand, at a high flow rate (7.2 mL min^{-1}), the residence period of metal ions in the column is short and thus U(VI) ions run away from the column before achievement of the equilibrium. This leads to decreasing U(VI) uptake capacity. When the process is subjected to external mass transfer control, a higher flow rate decreases the liquid film resistance and when the process is subjected to internal mass transfer control, a slower flow rate favors the biosorption. As the controlled-rate step shifted from external to internal mass transfer limitations, the uptake capacity of U(VI) reached to optimum point 223.58 mg g^{-1} in flow rate of 5.2 ml min^{-1}. This behavior is similar to what was seen in biosorption from single metal solutions. As obvious, when Fe(II) was added to the solution of U(VI), the breakthrough time (min) of U(VI) reduced from 333, 148 and 78 to 37, 34 and 20 for flow rate 3.2, 5.2 and 7.2 ml min^{-1}, respectively. Also, the uptake capacity of U(VI) (mg g^{-1}) for binary component system compared with single component system decreased from 337.29, 363.87 and 286.61 to 165.31, 223.58 and 199.95 for flow rate 3.2, 5.2 and 7.2 ml min^{-1}, respectively. Although the inlet molar concentration of Fe(II) ion is 15 times greater than inlet molar concentration of U(VI) ions, the uptake capacity of U(VI) decreased only 51%, 43% and 26% at flow rates of 3.2, 5.2 and 7.2 ml min^{-1}, respectively. The observed decrease in the biosorption of U(VI) in the presence of Fe(II) ions could be explained by the competition between metal ions for the same biosorption sites [29]. Similar to the single component system, the flow rate 5.2 ml min^{-1} was the optimum flow rate in binary component system.

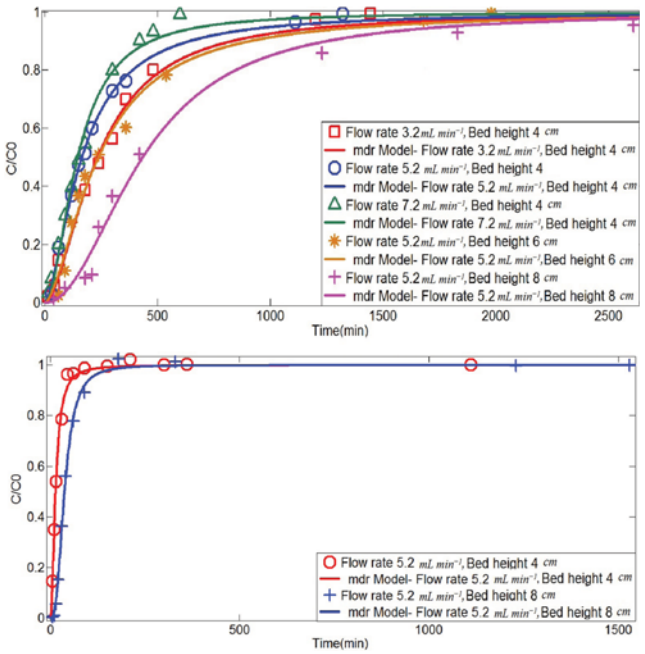

Fig. 2. Comparison of the experimental and predicted breakthrough curves for (a) U(VI) and (b) Fe(II) biosorption from binary-component system by Ca-pretreated *C. indica* at different bed heights and flow rates according to the Modified dose-response model (initial uranium(VI) concentration=250 mg l^{-1}; initial iron(II) concentration=900 mg l^{-1}; pH 4).

The breakthrough curves of the U(VI) metal biosorption from binary mixtures for various bed heights are shown in Fig. 2(a). The breakthrough time of the U(VI) reduced from 148, 319 and 643 to 34, 69 and 87 for the bed height 4,6 and 8 cm, respectively (Table 1). When Fe(II) was added to the solution of U(VI), the uptake capacity of uranium (mg g^{-1}) decreased from 363.87, 381.14 and 433.03 to 223.58, 227.14 and 257.21 for the bed height 4, 6 and 8 cm, respectively. Similar to the single component system, of the three bed heights tested, 8 cm gave the best results.

The breakthrough curves of Fe(II) were investigated for a binary component system in two conditions. These conditions include the flow rate 5.2 ml min^{-1} and bed heights 4 and 8 cm. The results of the experiments are shown in Figs. 2(b) and the results of the breakthrough curve analysis are given in Table 1. Initially, there are many active sites on Ca-pretreated *C. indica* biomass, so both U(VI) and Fe(II) are biosorbed by the algae. However, with the ongoing process, U(VI) progressively displaces Fe(II) ions that were previously biosorbed. The release of Fe(II) ions results in outlet concentrations of the metal that is higher than the concentrations of the feed solution. This observation is not rare in a multi-component system because of a chromatographic concentrating effect. These types of breakthrough curves (characterized by an overshoot) are indicative of the phenomenon of sequential exchange in which a more selective cation can remove another previously exchanged cation from the site. Similar results have been reported by other researchers [33-35].

Fig. 3 shows the breakthrough curves of U(VI) and Fe(II) on a Ca-pretreated *C. indica* biomass fixed-bed column in the binary

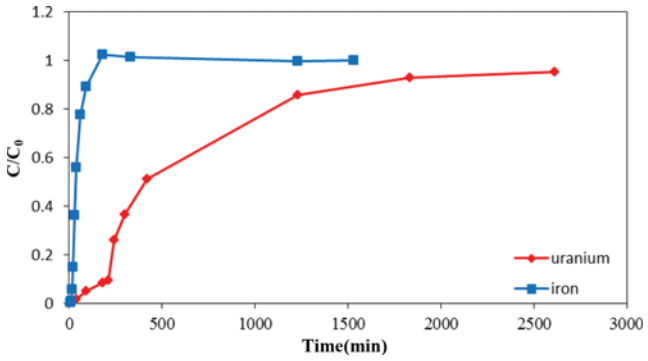

Fig. 3. Breakthrough curves of U(VI) and Fe(II) on a Ca-pretreated *C. indica* packed bed column in the binary-component system (bed heights=8 cm; flow rate=5.2 ml min^{-1}; pH 4).

system for flow rate 5.2 ml min^{-1} and bed height 8 cm. It could be seen that both of the two metal ions could be removed completely at the beginning. First, Fe(II) flowed out of the column at 5 min and was followed by U(VI) at the time of 27 min. The whole biosorption process could be divided into three phases: (1) complete biosorption phase (0-5 min)—both of the metal ions could be removed completely in this phase due to the large number of active sites; (2) separation phase (5-27 min)—with the occupation of the active sites, Fe(II) begun to flow out of the column, while U(VI) was still completely biosorbed by the modified biosorbents. The two metal ions could be separated totally in this phase; and (3) saturation phase (>27 min)—both of the metal ions flowed out of the column due to the full occupation of the active sites. Since Fe(II) first flowed out of the column in the binary system, the modified biosorbents had high biosorption affinity with U(VI). In a single component system under continuous condition, the uptake capacities were 433.03 and 73.49 mg g^{-1} for U(VI) and Fe(II), respectively. In a binary component system, the uptake capacity decreased to 257.21 and 62.04 mg g^{-1} for U(VI) and Fe(II). These results suggested that there was an antagonistic effect in the competitive biosorption process under the binary system. The Ca-pretreated *C. indica* biomass displayed a high selectivity toward one metal ion with an affinity order of U(VI)>Fe(II), which made it possible to separate the metal ions step by step through designing a proper experiment condition. The adsorption selectivity of the Ca-pretreated biomass may be improved by using the different complexing agents such as EDTA (ethylene diamine tetra ascetic acid) and sodium carbonate in the fixed-bed column.

Similar observations were reported by Yu et al. [36] for different binary component systems. Their dynamic competitive adsorption experiments showed that the modified leaf had higher adsorption affinity for Cu(II) than for Cd(II) and Zn(II) [36].

3. Study of Biosorption from Multi-metal Solutions

Since the real solutions often contain several metal ions simultaneously, the feasibility of Ca-pretreated *C. indica* for biosorption of U(VI) ion from real multi-metal solutions was also tested using uranium mining ore leach solutions of Saghand and Bandar Abbas of Iran. The compositions of these leach solutions are given in Table 2. Both simulated leach solutions were passed separately through the column in optimized conditions (bed height 8 cm and

Table 2. Concentration of metal ions in the leach solutions

Bandar Abbas leach solution	U	Fe	Zn	Co	Ni	Cu
Concentration (mg L^{-1})	251	700	18	3.5	12	27
Saghand leach solution	U	Fe	La	Ce	Y	Yb
Concentration (mg L^{-1})	243	830	1290	1080	1090	80

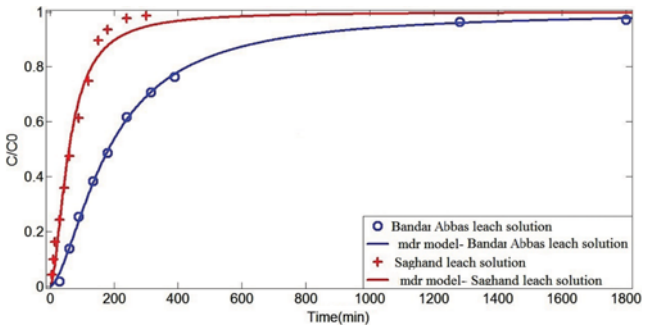

Fig. 4. Comparison of the experimental and predicted breakthrough curves for U(VI) biosorption from multi-component system by Ca-pretreated *C. indica* according to the modified dose-response model (bed heights=8 cm; flow rate=5.2 ml min^{-1}; pH 4).

flow rate 5.2 ml min^{-1}). The breakthrough curves of U(VI) biosorption from these multi-metal leach solutions are shown in Fig. 4 and the data analyses are given in Table 1. The breakthrough and exhaustion points are found to be premature as far as biosorption of U(VI) in multi-component system were concerned (Table 1). Also, the uptake capacity of U(VI) by Ca-pretreated *C. indica* biomass decreased when real solutions passed through the column. It was due to the presence of the considerable other kinds of heavy metal ions in the leach solutions which compete in occupying the binding sites. As can be seen from Table 1, the uptake capacity of U(VI) from Saghand leach solution compared with the single component system decreases from 433.03 to 30.09 mg g^{-1} (93% reduction). In the light of these results, it is concluded that the biosorbent was not found to be very efficient for the biosorption of U(VI) ions from real solution with high concentration of other metal ions. On the other hand, the uptake capacity of U(VI) from the Bandar Abbas leach solution is 130 mg g^{-1} which shows that Ca-pretreated *C. indica* can be fairly efficient for the biosorption of U(VI) ions.

4. Model of Column Data

The BDST model can be used to estimate the required bed depth for a given service-time. The model parameters were estimated by plotting of service time against the bed height at a flow rate of 5.2 ml min^{-1} for single and binary component systems, under which the effluent U(VI) concentration reached 12.5 mg l^{-1} (C/C_0=0.05). The equation of linear relationship was derived with R^2 value around 0.97. The rate constant (Ka) is 3.16×10^{-5} L mg^{-1} min^{-1} (single) and 7.28×10^{-4} L mg^{-1} min^{-1} (binary) and the biosorption capacity of the bed (N0) is 91,083 mg L^{-1} (single) and 9,752 mg L^{-1} (binary). The BDST model parameters can be useful to scale up the pro-

Table 3. Parameters obtained from the non-linear fit of breakthrough data to the Thomas and modified dose-response models for single, binary and multi-component systems

Experimental conditions			Thomas model			Modified dose-response model		
Metal	Q (ml min^{-1})	Z (cm)	q_0 (mg g^{-1})	q_0 (mg g^{-1})	R^2	a_{mdr}	b_{mdr} (*l*)	R^2
Single system								
U(VI)	3.2	4	270.9	270.9	0.98	4.111	1.795	0.99
	5.2	4	280.1	280.1	0.97	3.257	1.776	0.99
	7.2	4	260.7	260.7	0.99	3.172	1.737	0.99
	5.2	6	318.5	318.5	0.97	3.894	3.228	0.99
	5.2	8	411.6	411.6	0.99	5.721	5.467	0.99
Fe(II)	5.2	4	41.27	41.27	0.98	1.837	0.069	0.99
	5.2	8	51.01	51.01	0.96	1.884	0.175	0.99
Binary system								
U(VI)	3.2	4	121.3	121.3	0.98	1.736	0.751	0.99
	5.2	4	138.4	138.4	0.96	1.616	0.852	0.99
	7.2	4	171.8	171.8	0.98	1.877	1.053	0.99
	5.2	6	141.1	141.1	0.95	1.636	1.237	0.98
	5.2	8	180.1	180.1	0.95	2.075	2.260	0.99
Fe(II)	5.2	4	42.72	42.72	0.98	1.966	0.071	0.99
	5.2	8	52.79	52.79	0.98	2.749	0.194	0.99
Multi-component system								
Bandar Abbas leach solution, U(VI)	5.2	8	87.29	87.29	0.95	1.628	0.951	0.99
Saghand leach solution, U(VI)	5.2	8	28.9	28.9	0.98	1.771	0.308	0.98

cess for other flow rates without further experimental data.

The experimental data were fitted to the Thomas model to specify the uptake capacity (q_0) and model constant (k_{Th}) for single, binary and multi-component systems (Figure not shown). The model constants k_{Th} and q_0 along with correlation coefficients (R^2) for both metal ions are presented in Table 3. As the bed height increased in both metal ions, the value of k_{Th} decreased and the value of q_0 increased under both single and binary systems. Also, for both metal ions, the rate constant (k_{Th}) which characterizes the rate of solute transfer from the liquid to the solid phase and the maximum uptake capacity (q_0) increased with an increase in the flow rate for both single and binary systems. Similar observations were reported [18,37].

The best fits were seen when the modified dose-response model (Figs. 1, 2 and 4) was compared with the Thomas model as shown in Table 3, with correlation coefficients (R^2) above 0.98. Moreover, it can be seen that in most cases, the experimental uptake capacities are very close to those calculated by the modified dose-response model (Table 1). As can be seen, the values of a_{mdr} and b_{mdr} of dose-response model increase with increasing bed height, but with increasing flow rate, the values of a_{mdr} and b_{mdr} do not follow a specific trend. These results are in agreement with those obtained in the other references [26,38].

5. Biosorption Mechanism

To obtain information on the nature of possible interactions between the functional groups of Ca-pretreated *C. indica* biomass and the metal ions, a comparison between the FTIR spectra before

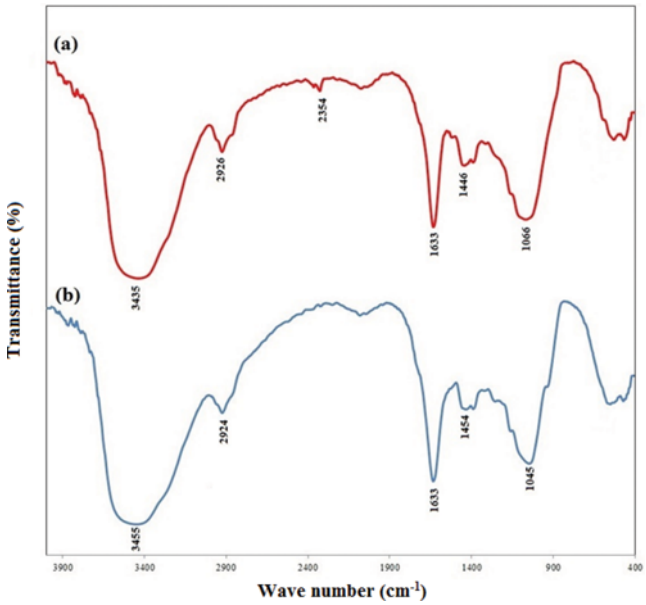

Fig. 5. FTIR analysis of Ca-pretreated *C. indica* algae before (a) and after (b) biosorption of U(VI) and Fe(II).

Table 4. Biosorption bands attributed to functional groups present in Ca-pretreated *C. indica*

Biosorption band	
Wave number (cm^{-1})	Vibration assignment
3435	Stretching of O-H bonds of hydroxyl groups from alcohols, phenols and carboxylic acids or stretching of NH_2 [39-41]
2926	Symmetric or asymmetric stretching of C-H bonds of aliphatic compounds [40,42]
2354	Stretching vibrations of N-H or stretching vibrations of C=O from ketones [43]
1633	Asymmetric Stretching of C=O bond from carboxylic acids or amides [39,43]
1446	Asymmetric Stretching of C=O bond from carboxylic acids [42]
1066	Stretching of C-OH bonds from alcohols or carboxylic acids [39,40]

and after biosorption of U(VI) and Fe(II) was made (Fig. 5). The shift of some functional group bands represents a functional group involved in the adsorption process. Table 4 shows the functional groups attributed to each biosorption band. The carboxylic groups are generally the most common acidic functional groups in the brown algae [7]. The peak at 1,446 cm^{-1} represents the carboxylate salt COO-M, where M defines the metal cations such as Na^+, K^+, Ca^{2+} and Mg^{2+} that may naturally exist in the biomass; also by modifying algae, calcium ions collect on the functional group. Henceforth, the ion-exchange mechanism is effective [44]. Based on similar studies, the carboxylate ions may coordinate with Fe(II) and U(VI) ions as chelating (bidentate) complexes [45]. Shifting frequency of the groups -OH, -NH_2 and -CO apparently binds these groups with U(VI) and Fe(II) through ion exchange mechanism, as well as the electrostatic forces of attraction between the negative charges of biosorbent surface and the positive charge of Fe(II) and U(VI) ions [46].

A comparison of the results of Fe(II) and U(VI) biosorption based on percentages changes, before and after the addition of biosorbent can reflect the qualitative transformation and migration mechanisms of the elements and enable us to speculate the biosorption mechanism of Fe(II) and U(VI) by Ca-pretreated *C. indica* biomass. The results of XRF analysis on Ca-pretreated *C. indica* biomass before and after biosorption of Fe(II) and U(VI) are shown in Table 5. As seen, after biosorption of Fe(II) and U(VI), the weight percentage of calcium element in the biomass decreased significantly. On the other hand, after biosorption of Fe(II) and U(VI), the contents of iron and uranium elements in the Ca-pretreated *C. indica* biomass increase from 1.6% and 0.0% to 20.91% and 52.36%, respectively. It confirms the replacement of calcium ion in binding sites with U(VI) and Fe(II) ions. This observation also proves that ion exchange is the main mechanism of metal ions biosorption by this biomass.

Table 5. XRF analysis on the Ca-pretreated *C. indica* before and after biosorption of U(VI) and Fe(II)

Element	wt%	
	Before biosorption	After biosorption
MgO	1.16	0.00
Al_2O_3	3.45	1.38
SiO_2	16.57	7.54
P_2O_5	0.78	0.00
SO_3	19.73	8.50
Cl	0.31	0.97
K_2O	0.76	0.47
CaO	49.81	3.87
TiO_2	0.21	0.12
Fe_2O_3	1.60	20.91
Zn	0.39	0.00
Br	1.03	0.12
Sr	0.90	0.31
I	0.17	0.26
UO_2	0.00	52.36
ZrO_2	0.14	0.28

The amounts of the Ca(II) ion released from the Ca-pretreated *C. indica* algae and pH of effluent stream vs. time for single component system of U(VI) with inlet concentration 250 mg L^{-1}, flow rate 5.2 ml min^{-1} and bed height 6 cm are shown in Fig. 6. During the biosorption in the packed bed column, Ca(II) ions deposited in the algal biomass were observed to be released considerably. Since the binding affinity between the functional groups and U(VI) ions is greater than that between Ca(II) ions and functional groups, the release of Ca(II) ions suggests again that ion exchange could play a significant role as a biosorption mechanism as the U(VI) ions could replace Ca(II) in the algal structure. As shown in Fig. 6, in the period of time before breakthrough of U(VI) biosorption (319 min), the U(VI) was adsorbed onto *C. indica* almost efficiently

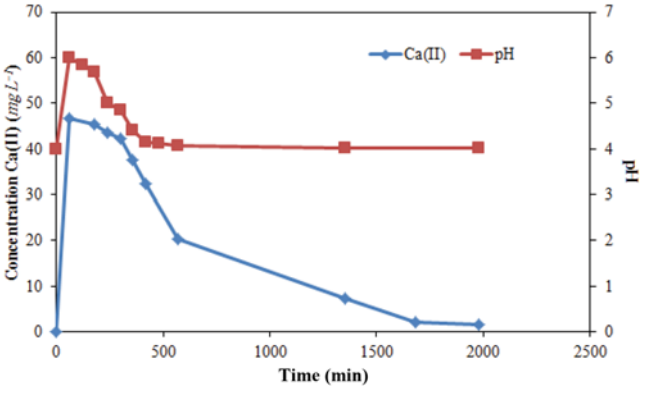

Fig. 6. Profile of calcium ion concentration and pH from effluent column (inlet concentration of U(VI) 250 mg L^{-1}, flow rate 5.2 ml min^{-1} and bed height 6 cm).

and the amount of Ca(II) ions in the effluent stream was high showing no obvious variation. After breakthrough time of U(VI) biosorption, concurrent with the decreasing of biosorption rate, the amount of Ca(II) ions in the effluent stream reduced rapidly and the concentration of Ca(II) approached to zero in the exhaustion time of biosorption process. This result was confirmed with a pH diagram. As can be seen, the pH of solution increased rapidly as the Ca(II) ions increased in effluent stream. Then, by reduction in calcium binding sites as well as by a decrease in biosorption rate, the effluent pH decreased gradually until the effluent pH became equal to the influent pH (about 4) at the point of complete exhaustion of the biosorption bed. Ion exchange has been considered to be the main biosorption mechanism by many researchers [8,13,32].

CONCLUSIONS

Biosorption of uranium and iron by Ca-pretreated *Cystoseira indica* biomass was studied using a continuous packed bed column. Breakthrough profiles were obtained at different bed heights and flow rates. The results indicate that the maximum uptake capacity of U(VI) biosorption, 433.03 and 257.21 mg g^{-1} for single and binary component systems, respectively, was obtained at flow rate of 5.2 ml min^{-1} and bed height of 8 cm. As the controlled-rate step shifted from external to internal mass transfer limitations, the flow rate of 5.2 ml min^{-1} with an optimum uptake capacity of U(VI) was created. During the column testing, the reduction in uptake capacity of the biomass in the binary component systems compared to single component systems refers to an antagonistic effect. Due to the difference in the biosorption affinity, the whole process could be divided into three phases: complete biosorption phase, separation phase and saturation phase. The results show that the algal biomass had a higher affinity for U(VI) ions than for Fe(II) ions; consequently, an overshoot on Fe(II) breakthrough profiles was manifested. Also, it was observed that the uptake capacity of U(VI) from leach solutions compared with the single component system decreased dramatically.

BDST model well correlated the relationship between service time and bed height for U(VI) and iron (II) biosorption in a packed bed of biomass, which is essential in column process design. On the other hand, the modified dose-response model compared with the Thomas model can successfully predict the breakthrough profiles specified under varying experimental conditions. The constants of these models were obtained with high regression coefficients greater than 0.98.

FTIR studies show that most effective mechanisms in the U(VI) and Fe(II) biosorption processes could be determined as an ion-exchange, electrostatic interaction and complexation. Also, the ion exchange was confirmed to be one of the main mechanisms responsible for U(VI) and Fe(II) biosorption according to XRF analysis before and after biosorption and monitoring of pH and Ca(II) concentration in the column effluent.

ACKNOWLEDGEMENTS

This project was financially supported by Nuclear Science and Technology Research Institute, Atomic Energy Organization of Iran.

NOMENCLATURE

a_{mdr} : modified dose-response model constant
b_{mdr} : modified dose-response model constant
C_0 : input concentration [mg L^{-1}]
C_b : breakthrough concentration [mg/L]
C_t : outlet concentration [mg L^{-1}]
K_a : rate constant [L mg^{-1} min^{-1}]
k_{Th} : thomas rate constant [L min^{-1} g^{-1}]
M_{total} : total amount of metal sent to column [g]
m_s : dry weight of biosorbent [g]
N_0 : biosorption capacity of the bed [mg L^{-1}]
Q : flow rate [mL min^{-1}]
q_{total} : uptake capacity [mg metal g^{-1} biosorbent]
q_0 : the maximum uptake capacity [mg g^{-1}]
T : time [min]
t_b : breakthrough time [min]
t_e : exhaustion time [min]
V : volume [*l*]
Ve : effluent volume [mL]
v : linear velocity [cm min^{-1}]
Z : bed height [cm]

REFERENCES

1. O. D. Uluozlu, M. Tuzen, D. Mendil and M. Soylak, *J. Hazard. Mater.*, **176**, 1032 (2010).
2. G. Ciardelli, L. Corsi and M. Marcucci, *Resour. Conserv. Recycl.*, **31**, 189 (2001).
3. G. Chen, *Sep. Purif. Technol.*, **38**, 11 (2004).
4. U. Ipek, *Desalination*, **174**, 161 (2005).
5. A. Borowiak-Resterna, R. Cierpiszewski and K. Prochaska, *J. Hazard. Mater.*, **179**, 828 (2010).
6. A. M. Shoushtari, M. Zargaran and M. Abdouss, *J. Appl. Polym. Sci.*, **101**, 2202 (2006).
7. T. A. Davis, B. Volesky and A. Mucci, *Water. Res.*, **37**, 4311 (2003).
8. K. Naddafi, R. Nabizadeh, R. Saeedi, A. H. Mahvi, F. Vaezi, K. Yaghmaeian, A. Ghasri and S. Nazmara, *J. Hazard. Mater.*, **147**, 785 (2007).
9. B. Kiran and A. Kaushik, *Chem. Eng. J.*, **144**, 391 (2008).
10. S. Mona, A. Kaushik and C. P. Kaushik, *Ecol. Eng.*, **37**, 1589 (2011).
11. K. Vijayaraghavan, J. Jegan, K. Palanivelun and M. Velan, *Sep. Purif. Technol.*, **44**, 53 (2005).
12. V. J. Vilar, C. Botelho and R. A. Boaventura, *Chem. Eng. J.*, **144**, 420 (2008).
13. M. Riazi, A. R. Keshtkar and M. A. Moosavian, *J. Radioanal. Nucl. Chem.*, **301**, 493 (2014).
14. A. R. Keshtkar and M. A. Hassani, *Korean J. Chem. Eng.*, **31**, 289 (2014).
15. M. Ghasemi, A. R. Keshtkar, R. Dabbagh and S. Jaber Safdari, *J. Hazard. Mater.*, **189**, 141 (2011).
16. V. Diniz, M. E. Weber, B. Volesky and G. Naja, *Water Res.*, **42**, 363 (2008).
17. K. H. Chu, *Chem. Eng. J.*, **97**, 233 (2004).
18. C. M. Futalan, C. C. Kan, M. L. Dalida, C. Pascua and M. W. Wan, *Carbohydr. Polym.*, **83**, 697 (2011).

19. Z. Zulfadhly, M. D. Mashitah and S. Bhatia, *Environ. Pollut.*, **112**, 463 (2001).
20. K. Vijayaraghavan, J. Jegan, K. Palanivelu and M. Velan, *J. Hazard. Mater.*, **113**, 223 (2004).
21. H. Muhamad, H. Doan and A. Lohi, *Chem. Eng. J.*, **158**, 369 (2010).
22. H. C. Thomas, *Ann. N.Y. Acad. Sci.*, **49**, 161 (1948).
23. P. Suksabye, P. Thiravetyan and W. Nakbanpote, *J. Hazard. Mater.*, **160**, 56 (2008).
24. G. Yan, T. Viraraghavan and M. Chen, *Adsorpt. Sci. Technol.*, **19**, 25 (2001).
25. J. Song, W. Zou, Y. Bian, F. Su and R. Han, *Desalination*, **265**, 119 (2011).
26. A. Singh, D. Kumar and J. P. Gaur, *Water Res.*, **46**, 779 (2012).
27. D. C. Ko, J. F. Porter and G. McKay, *Chem. Eng. Sci.*, **55**, 5819 (2000).
28. V. C. Taty-Costodes, H. Fauduet, C. Porte and Y. S. Ho, *J. Hazard. Mater.*, **123**, 135 (2005).
29. K. U. Ahamad and M. Jawed, *Desalination*, **285**, 345 (2012).
30. R. Flouty and G. Estephane, *J. Environ. Manage.*, **111**, 106 (2012).
31. Y. Wang, H. Gao, J. Sun, J. Li, Y. Su, Y. Ji and C. Gong, *Desalination*, **270**, 258 (2011).
32. A. H. Hawari and C. N. Mulligan, *Process Biochem.*, **42**, 1546 (2007).
33. S. J. Kleinübing, E. Guibal, E. A. Da Silva and M. G. C. Da Silva, *Chem. Eng. J.*, **184**, 16 (2012).
34. Y. Zhang and C. Banks, *Water Res.*, **40**, 788 (2006).
35. C. Escudero, J. Poch and I. Villaescusa, *Chem. Eng. J.*, **217**, 129 (2013).
36. J. X. Yu, L. Y. Feng, X. L. Cai, L. Y. Wang and R. A. Chi, *Environ. Earth Sci.*, **73**, 1789 (2015).
37. K. S. Rao, S. Anand and P. Venkateswarlu, *J. Ind. Eng. Chem.*, **17**, 174 (2011).
38. S. V. Gokhale, K. K. Jyoti and S. S. Lele, *J. Hazard. Mater.*, **170**, 735 (2009).
39. A. García-Mendieta, M. T. Olguín and M. Solache-Ríos, *Desalination*, **284**, 167 (2012).
40. M. Iqbal, A. Saeed and S. I. Zafar, *J. Hazard. Mater.*, **164**, 161 (2009).
41. M. A. Wahab, S. Jellali and N. Jedidi, *Bioresour. Technol.*, **101**, 5070 (2010).
42. A. Sarı and M. Tuzen, *J. Hazard. Mater.*, **160**, 349 (2008).
43. N. V. Farinella, G. D. Matos and M. A. Z. Arruda, *Bioresour. Technol.*, **98**, 1940 (2007).
44. V. Murphy, H. Hughes and P. McLoughlin, *Water Res.*, **41**, 731 (2007).
45. K. Nakamoto, *Infrared and Raman spectra of inorganic and coordination compounds*, John Wiley & Sons, Ltd. (1978).
46. H. A. Hasan, S. R. S Abdullah, N. T. Kofli and S. K. Kamarudin, *J. Environ. Manage.*, **111**, 34 (2012).